ISSN Print: 0976-6340 ISSN Online: 0976-6359

INTERNATIONAL JOURNAL OF MECHANICAL ENGINEERING & TECHNOLOGY (IJMET)

https://iaeme.com/Home/journal/IJMET

High Quality Peer Reviewed Refereed Scientific, Engineering & Technology, Medicine and Management International Journals

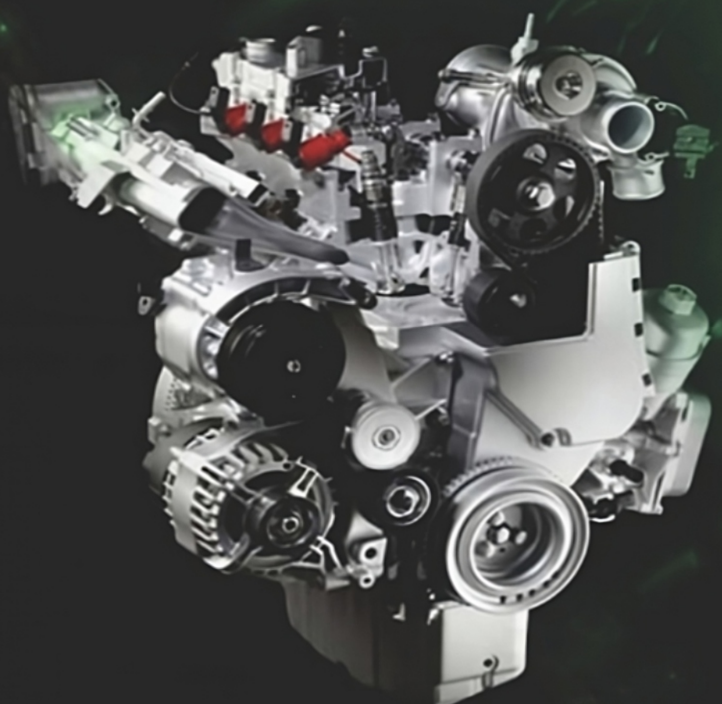

PUBLISHED BY

IAEME Publication
Chennai, Tamilnadu, India
Mobile: +91-9884798314, 7358208318
E-mail: iaemedu@gmail.com, editor@iaeme.com

International Journal of Mechanical Engineering and Technology (IJMET)
Volume 16, Issue 3, May-June 2025, pp. 67-87, Article ID: IJMET_16_03_004
Available online at https://iaeme.com/Home/issue/IJMET?Volume=16&Issue=3
ISSN Print: 0976-6340; ISSN Online: 0976-6359; Journal ID: 4544-4179
Impact Factor (2025): 20.99 (Based on Google Scholar Citation)
DOI: https://doi.org/10.34218/IJMET_16_03_004

SCOPE DATABASE INDEXED

OPEN ACCESS

PERFORMANCE ANALYSIS OF SURFACE TEXTURED HYDRODYNAMIC JOURNAL BEARING UNDER INFLUENCE OF NON-NEWTONIAN LUBRICANT

Kushare Dnyaneshwar V [1*] and Soni Sandeep [2]

[1] Department of Mechanical Engineering, MVPS's College of Engineering, Nashik, India.

[2] Department of Mechanical Engineering, SVNIT, Surat, Gujarat, India.

[*] **Corresponding author: Kushare Dnyaneshwar V**

ABSTRACT

The operating and geometric parameters of textures affect the static, dynamic, and stability performance characteristics of a hydrodynamic journal-bearing system. The present work investigates the influence of spherical textures on the performance parameters of a hydrodynamic journal bearing system. The flow of a lubricant is assumed to be Non-Newtonian and Reynolds's equation governing the flow of a lubricant between the space in the bearing and the journal is solved by a finite-element method (FEM). The computed results indicate that the spherically textured two lobe hydrodynamic journal bearing provides better improvement in the performance parameters than two lobe hydrodynamic journal bearing with plain surface.

Keywords: Textured geometry, Lobe bearing, Non-Newtonian lubricants, hydrodynamic lubrication, and load carrying capacity.

Cite this Article: Kushare Dnyaneshwar V and Soni Sandeep. (2025). Performance Analysis of Surface Textured Hydrodynamic Journal Bearing under Influence of Non-Newtonian Lubricant. *International Journal of Mechanical Engineering and Technology (IJMET)*, 16(3), 67-87.

https://iaeme.com/MasterAdmin/Journal_uploads/IJMET/VOLUME_16_ISSUE_3/IJMET_16_03_004.pdf

1. INTRODUCTION

Over the past decade lot of research have been done in the field of textured hydrodynamic journal bearing. In textured bearing micro textures are created on the inner surface of bearing which enhance the performance characteristics of the hydrodynamic journal bearing. Non circular bearing are known to have better performance characteristics as compared circular hydrodynamic journal bearing. The different configuration in non-circular bearing are offset halve bearing, two lobe bearing, three lobe bearing and four lobe bearing. This research paper presents comprehensive static and dynamic performance data for spherical textured two lobe hydrodynamic journal bearing. Micro texturing the inner surface of a hydrodynamic journal bearing provides an additional clearance between the journal and bearing surface. The textured area acts as a lubricant reservoir and increases the lubricant film thickness.

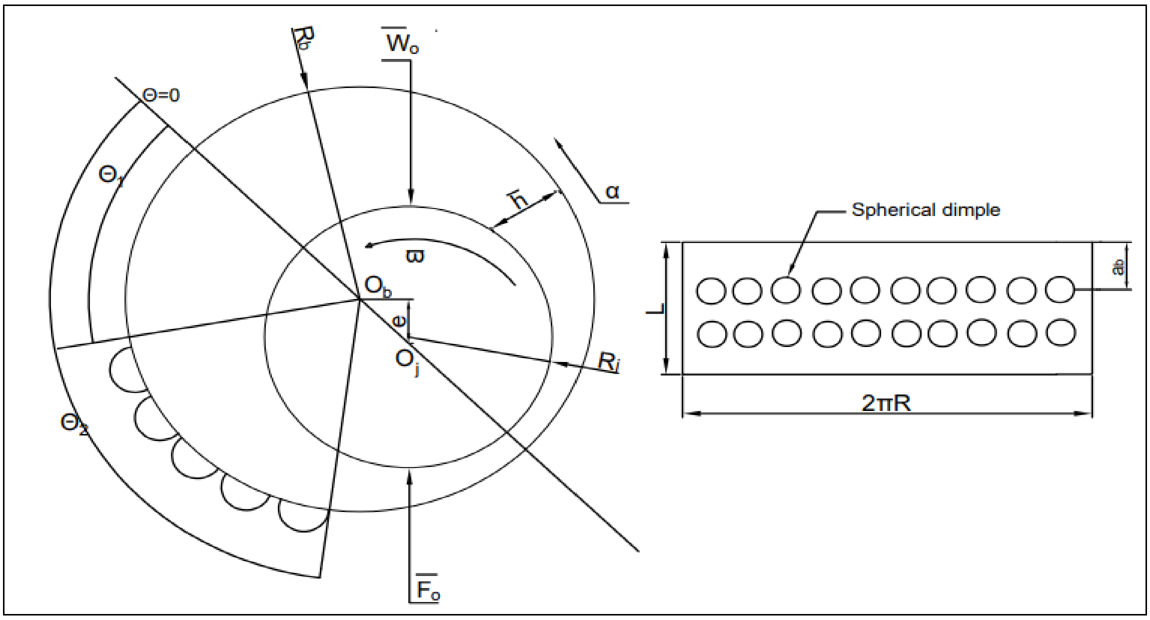

(a)

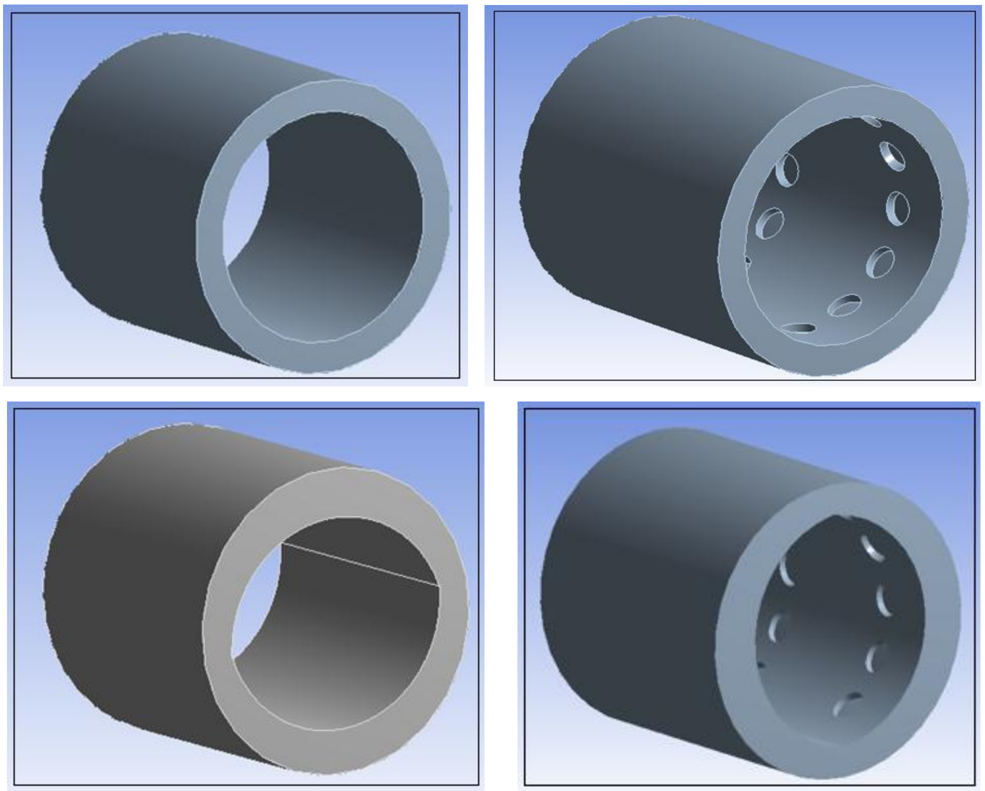

(b)

Figure 1: (a) Textured circular bearing configuration (b) Plain and textured circular / Two lobe hydrodynamic journal bearing configuration

N Tala-Ighil et.al. [1] Studied the effect of surface textures on the lubrication of a hydrodynamic journal-bearing under steady-state conditions by finite-difference numerical method. The bearing surface is numerically textured with spherical dimples. The numerical results indicate that textures affect the most important bearing characteristics: film thickness, pressure distributions, axial film flow, and frictional torque. In this research work author concluded that spherically textured surfaces with appropriate geometrical parameter such as size, depth, and number of dimples may affect bearing characteristics. N Tala-Ighil et.al. [2] The textures distribution influence on the bearing surface of a hydrodynamic journal bearing subjected to a stationary load studied by finite element numerical model. The bearing surface is partially or totally textured with cylindrical dimples. Different arrangements of the textured area have been considered. The presence of a texture increases locally the lubricant film thickness and decreases the friction force. The author concluded that full texturing appears ineffective to generate hydrodynamic load capacity in the contact by the cavitation effects. Partial texturing can generate hydrodynamic lift in bearing, when the texture is located in the declining part of the contact pressure field. F.M. Meng et.al. [3] In the present study fluid structure interaction (FSI) method is used for the numerical analysis of compound textured hydrodynamic journal bearing. The rectangular–spherical dimple is used for compound texture. The compound texture's effect on the tribological performances for the hydrodynamic journal bearing is investigated. The major conclusion is that the compound textures shows a better behavior in increasing the load carrying capacity and lowering the friction coefficient of the journal bearing, as compared with the simple texture. Chandra B. Khatri et.al. [4] In the present work, the combined influence of micro-dimple textured surface and behavior of non-Newtonian lubricant on the performance of non-recessed hybrid journal bearing have been studied. On the basis of numerically simulated results computed in the present study, the major conclusions is that the value of minimum fluid film thickness is reduced by surface texturing of hole-entry hybrid journal bearing lubricated by lubricants such as pseudoplastic, Newtonian lubricant and dilatant. Chandra B. Khatri et.al. [5] in this research paper, a theoretical investigation dealing with the combined influence of textured surface and behavior of couple stress lubricant on the performance of slot-entry circular and two-lobe hybrid journal bearing have been investigated. Based on the simulated results covered in preceding sections, the following salient observations have been reported: The general interpretation of the numerically simulated results indicate that the presence of couple stress additives in base oil lubricant and surface texturing on the bearing surface predicts improved performance characteristics than the non-textured bearing lubricated with Newtonian lubricant for both circular and two-lobe slot entry hybrid journal bearing. Satish C. Sharma et.al. [6] The influence of Electro rheological fluid effects, caused by the applied electric field, on the three-lobe textured hole- entry journal bearings is quite significant. On the basis of the result discussed, the major conclusions drawn are. The textured hole-entry journal bearing reduces the value of minimum fluid film thickness relative to non-textured journal bearing. However, the use of ER fluid lubrication and three-lobe profile in textured hole-entry hybrid journal bearing gives higher values of minimum fluid film thickness over the Newtonian fluid lubricated circular non-textured journal bearing. It means the Electro rheological fluid lubricated smart three-lobe textured journal bearing can sustain higher value of external load than that of non-textured circular journal bearing lubricated with Newtonian fluid. Sanjay Sharma et.al. [7] Based upon the obtained numerical results, it has been observed that. Partial texturing can enhance the bearing performance, provided the texture zone is located in the increasing pressure region. Also, surface texturing has a pronounced effect on the bearing performance enhancement, when the bearing operates at lower eccentricities and the positive effects obtained from surface texturing diminish as the operating eccentricity ratio is increased. So, the partially textured bearing is efficient only for low or average journal eccentricity ratio, the best performance enhancement being obtained at the lowest eccentricity ratio it is also concluded that, for the triangular shaped texture, considered in the present study, the optimum values of texture depth and texture distribution region have also been determined. While designing, designers should focus on those values of texture depth, texture region and number of textures, which give the maximum value of performance enhancement ratio. Sanjay Sharma et.al. [8] In the present numerical-based study, the effect of triangular- shaped textures, with different texture depths and texture locations on the dynamic performance characteristics of hydrodynamic journal bearing has been investigated. The study has been done considering the hydrodynamic bearing operation under a moderate eccentricity ratio of 0.6. Moreover, for the triangular shaped texture considered in the present study, the optimum values of texture depth and number of textures have also been determined for maximum bearing dynamic performance.

2. Analysis

The governing non-dimensional Reynolds equation for a hydrodynamic journal bearing system for a laminar flow of isoviscous Non- Newtonian Lubricant in the convergent area of a journal and bearing system is expressed as [4,10].

$$\frac{\partial}{\partial\alpha}\left(\bar{h}^{3}\bar{F}_{2}\frac{\partial\bar{P}}{\partial\alpha}\right)+\frac{\partial}{\partial\beta}\left(\bar{h}^{3}\bar{F}_{2}\frac{\partial\bar{P}}{\partial\beta}\right)=\Omega\left[\frac{\partial}{\partial\alpha}\left\{\left(1-\frac{\bar{F}_{1}}{\bar{F}_{0}}\right)\bar{h}\right\}\right]+\frac{\partial\bar{h}}{\partial\bar{t}} \qquad (1)$$

Where $\bar{F}_0$ $\bar{F}_1$ and $\bar{F}_2$ are the cross apparent viscosity integral and calculated as follows

$$\bar{F}_0=\int_0^1\frac{1}{\bar{\mu}}d\bar{z}\ ;\quad \bar{F}_1=\int_0^1\frac{\bar{z}}{\bar{\mu}}d\bar{z}\ ;\quad \bar{F}_2=\int_0^1\frac{\bar{z}}{\bar{\mu}}\left(\bar{z}-\frac{\bar{F}_1}{\bar{F}_0}\right)d\bar{z}$$

The Reynolds equation (1) is solved using FEM, which is described below.

2.1 Fluid film thickness

The fluid film thickness for spherical textured journal bearing is expressed in non-dimensional form as [4]

$$\bar{h}_d=\begin{cases}\left[\left(\frac{\bar{h}_d}{2}+\frac{\bar{\delta}^2}{2\bar{h}_p}\right)^2-\bar{\delta}^2\left(\bar{x}_l^2+\bar{z}_l^2\right)\right]^{1/2}-\left[\left(\frac{\bar{\delta}^2}{2\bar{h}_p}-\frac{\bar{h}_p}{2}\right)\right] & r'<r_p\\ 1 & r'>r_p\end{cases} \qquad (2)$$

Where $\bar{\delta} = \frac{r_p}{h_r}, \bar{x} = \frac{x}{r_p}, \bar{z} = \frac{z}{r_p}, r^2 = \sqrt{\left(\bar{x}_l^2 + \bar{z}_l^2\right)}$

The nominal fluid film thickness for a two lobe hydrodynamic journal bearing is given by following equation in the non-dimensional form [5, 13]

$$\bar{h} = \frac{1}{\bar{\delta}} - (\bar{X}_J - \bar{X}_L^i)\cos\alpha - (\bar{Z}_J - \bar{Z}_L^i)\sin\alpha$$ (Plain two lobe hydrodynamic Journal bearing) (3)

$$\bar{h} = \frac{1}{\bar{\delta}} - (\bar{X}_J - \bar{X}_L^i)\cos\alpha - (\bar{Z}_J - \bar{Z}_L^i)\sin\alpha + \bar{h}_d$$ (Textured two lobe hydrodynamic Journal bearing) (4)

Where $\bar{X}_J = \varepsilon \sin\varphi$ and $\bar{Z}_J = -\varepsilon \cos\varphi$

2.2 Finite element formulation

The flow field has been discretized using four nodded quadrilateral elements. The equation for liner pressure over an element and is written as [5, 7]

$$\bar{P} = \sum_{j=1}^{n_i^e} \bar{P}_j N_j \tag{5}$$

Where N_j is the shape function and n_i^e is the number of nodes per element. Using Galerkin's and FEM method, the global system of equations can be written as follows [4, 10]

$$\left|\bar{F}\right|^e \left\{\bar{P}\right\}^e = \left\{\bar{Q}\right\}^e + \Omega\left\{\bar{R}_H\right\}^e + \dot{\bar{X}}_J \left\{\bar{R}_{Xj}\right\}^e + \dot{\bar{Z}}_J \left\{\bar{R}_{Zj}\right\}^e \tag{6}$$

2.3. Performance characteristics

The static performance characteristics are lubricant flow, load carrying capacity, frictional torque, minimum fluid-film thickness and dynamic performance characteristics fluid film dynamic coefficients and stability threshold speed.

2.3.1. Static performance characteristics

Using the steady state condition (i.e., $\bar{X}_J = \bar{Z}_J = 0$) of loading, the static performance characteristics are evaluated for a given vertical external load ($\bar{W}_0$)

Load carrying capacity.

The components of load carrying capacity are given as [29]

$$\overline{F}_x = -\int_{-\lambda}^{\lambda}\int_0^{2\pi} \overline{p}\cos\alpha \; d\alpha \; d\beta$$

$$\overline{F}_z = -\int_{-\lambda}^{\lambda}\int_0^{2\pi} \overline{p}\sin\alpha \; d\alpha \; d\beta \qquad (7)$$

The resultant load carrying capacity is expressed as

$$\overline{F} = \left[\overline{F}_x^2 + \overline{F}_z^2\right]^{1/2} \qquad (8)$$

2.3.2 Dynamic performance characteristics

Fluid-film stiffness coefficients.

The fluid-film stiffness coefficients are expressed as [25]

$$\overline{S}_{ij} = -\frac{\partial \overline{F_i}}{\partial \overline{q}} \; (i = x, z) \qquad (9)$$

Fluid-film damping coefficients.

The fluid-film damping coefficients are expressed as [25]

$$\overline{C}_{ij} = -\frac{\partial \overline{F_i}}{\partial \dot{\overline{q}}} \; (i = x, z) \qquad (10)$$

Stability parameters.

The linearized motion equation for the journal is written in the non-dimensional form as [24]

$$\left[\overline{M}_j\right]\left\{\ddot{\overline{X}}_J\right\} + \left[\overline{C}\right]\left\{\dot{\overline{X}}_J\right\} + \left[\overline{S}\right]\left\{\overline{X}_J\right\} = 0 \qquad (11)$$

The above motion equation may be expressed in matrix form as [ ]

$$\begin{bmatrix} \overline{M}J & 0 \\ 0 & \overline{M}j \end{bmatrix}\begin{Bmatrix} \ddot{\overline{X}}J \\ \ddot{\overline{Z}}J \end{Bmatrix} + \begin{bmatrix} \overline{C}xx & \overline{C}xz \\ \overline{C}zx & \overline{C}zz \end{bmatrix}\begin{Bmatrix} \dot{\overline{X}}J \\ \dot{\overline{Z}}J \end{Bmatrix} + \begin{bmatrix} \overline{S}xx & \overline{S}xz \\ \overline{S}zx & \overline{S}zz \end{bmatrix}\begin{Bmatrix} \overline{X}J \\ \overline{Z}J \end{Bmatrix} = \begin{Bmatrix} 0 \\ 0 \end{Bmatrix}$$

The non-dimensional value of critical mass ($\overline{M_c}$) for the journal is given by

$$\overline{M_c} = \frac{\overline{G_1}}{G_2 - G_3}$$

Where $\overline{G}_1 = \left[\overline{C}_{xx}\overline{C}_{zz} - \overline{C}_{zx}\overline{C}_{xz}\right]$, $\overline{G}_2 = \frac{\left[\overline{S}_{xx}\overline{S}_{zz} - \overline{S}_{zx}\overline{S}_{xz}\right]\left[\overline{C}_{xx} + \overline{C}_{zz}\right]}{\left[\overline{S}_{xx}\overline{C}_{zz} + \overline{S}_{zz}\overline{C}_{xx} - \overline{S}_{xz}\overline{C}_{zx} - \overline{S}_{zx}\overline{C}_{xz}\right]}$,

$$\overline{G}_3 = \frac{\left[\overline{S}_{xx}\overline{C}_{xx} + \overline{S}_{xz}\overline{C}_{xz} + \overline{S}_{zx}\overline{C}_{zx} + \overline{S}_{zz}\overline{C}_{zz}\right]}{\left[\overline{C}_{xx} + \overline{C}_{zz}\right]}$$

The threshold speed margin is given by

$$\overline{\omega_{th}} = \left[\overline{M}_C \big/ \overline{F_0}\right]^{1/2} \tag{12}$$

Boundary conditions

For two lobe hydrodynamic journal bearing the following boundary conditions are used [24]

1. Nodes on the boundary of bearing have absolute zero pressure.
2. Pressure gradient is zero.
3. Pressure at leading edge is considered to be atmospheric

2.4. Solution Procedure

The detail procedure for numerical analysis for the computation of performance characteristics of two lobe textured hydrodynamic journal bearing is shown in the figure.2 The Reynolds equation is solved by finite element method the accuracy of FEM is depends upon convergence study of finite element method. To find the solution of FEM equation, mesh size of 49x20 quadrilateral isoperimetric element is selected. The nominal fluid film thickness is calculated for two lobe textured and two lobe smooth hydrodynamic journal bearing for the given value of eccentricity ratio, using steady state conditions. To find the performance parameter of textured bearing for Newtonian lubricant a MATLAB code is developed. Once the convergence criterion is achieved, the program is terminated and performance characteristics are evaluated.

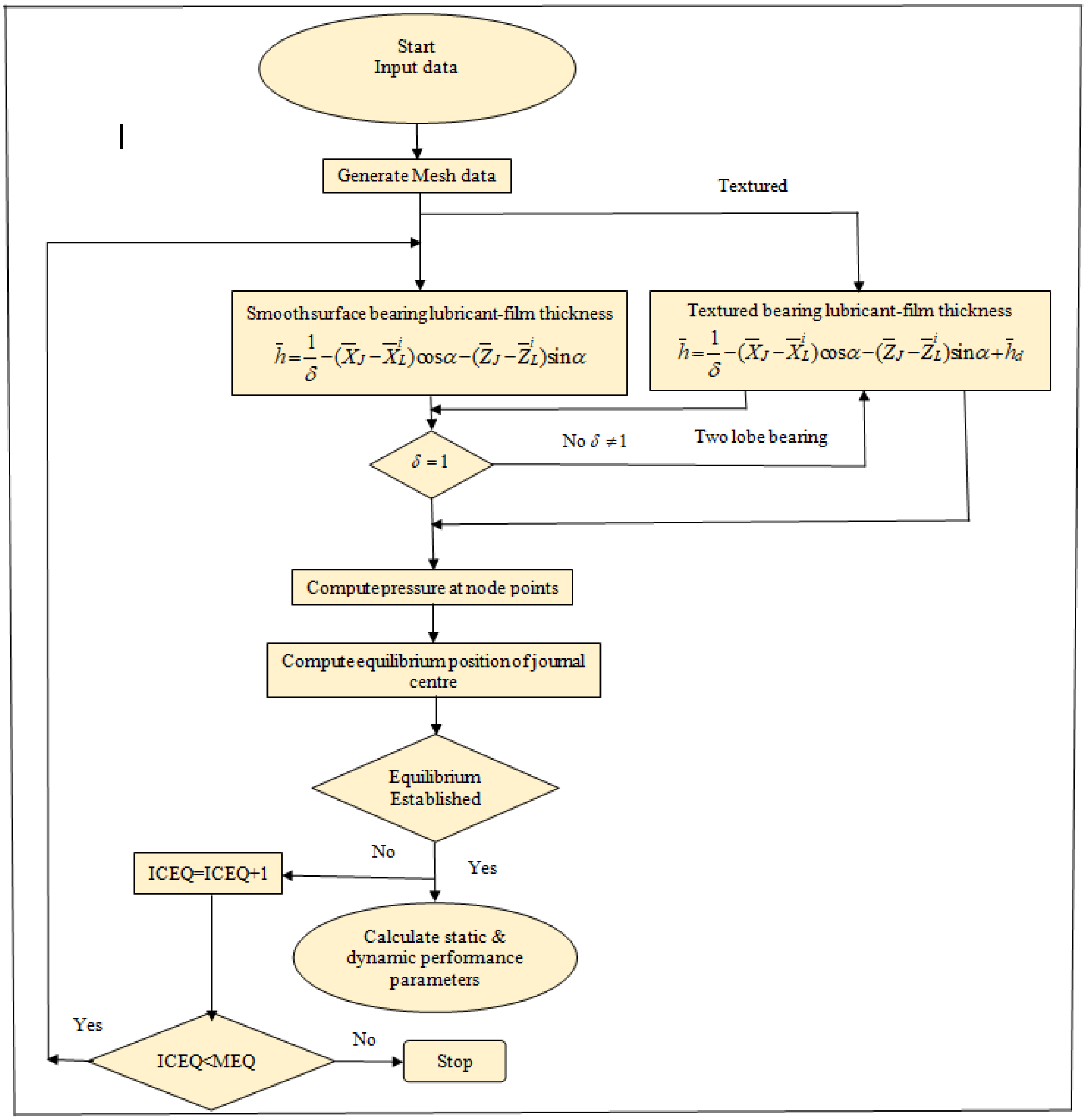

Figure 2: Solution Scheme

3. RESULTS AND DISCUSSION

The static and dynamic performance characteristics of two lobe hydrodynamic journal bearings having spherical micro textures are evaluated theoretically. In this study, non-dimensional value of texture radius ($\bar{r}_p$) is decided as 0.6.to evaluate the performance of textured journal bearing. The working and geometric parameters are as follows. To confirm the validity of the developed solution strategy, numerical model and MATLAB code the present results have been validated with the results of Khatri C.B. & S.C. Sharma [20] and Wang, X.L. & K.Q. Zhu [21]as shown in figure 4.

Table: 1. Working and geometric parameter used in this study.

Sr. No.	Parameters	Non dimensional value
1.	speed parameter (Ω)	1.0
2.	Eccentricity ratio (ε)	0.1 to 0.8
3.	Clearance ratio (Cr)	0.001
4.	Aspect ratio (L/D)	1.0
5.	Offset factor (δ)	0.8 ,1.0,1.25
6.	Shape of micro texture	Spherical
7.	Fully textured-I (θ)	0° to 360°
8.	No. of textures in circumferential direction ($N_{c\theta}$)	12
9.	No. of textures in Axial direction ($N_{a\theta}$)	2
10.	No. of Nodes in circumferential direction	49
11.	No. of Nodes in axial direction	20
12..	No. of elements	912
13.	Texture base radius ($\bar{r}_p$)	0.6
14.	Texture depth ($\bar{h}_d$)	0.2 to 1.3

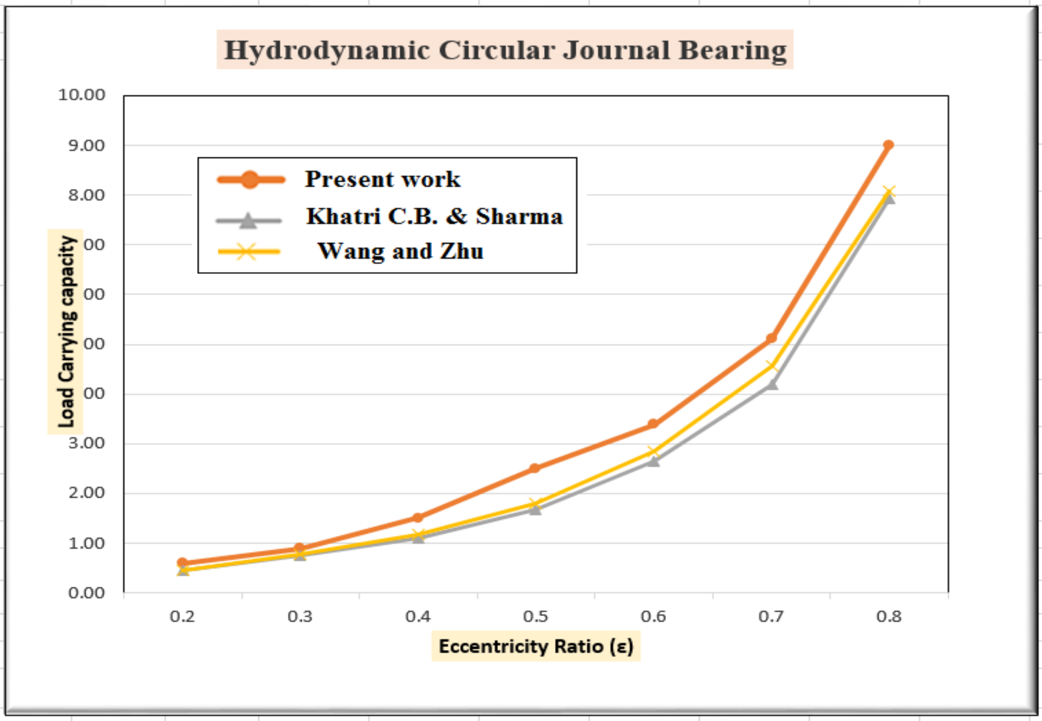

Figure 3. Validation of load carrying capacity ($\bar{F}_0$) versus eccentricity ratio (ε).

3.1 Load carrying capacity ($\bar{F}_0$).

The variation in non-dimensional value of load carrying capacity ($\bar{F}_0$) of plain circular, plain two lobe and textured circular, two lobe journal bearing versus eccentricity ratio (ε) is shown in figure 4. The load carrying capacity ($\bar{F}_0$) of textured circular and two lobe journal bearings is greater than plain journal bearing because of the change in fluid–film thickness of lubricant due to the presence of textures on the bearing surface, which in turn increases the hydrodynamic lift. The results indicate that the location of textures could play a significant role from the view point of load carrying capacity.

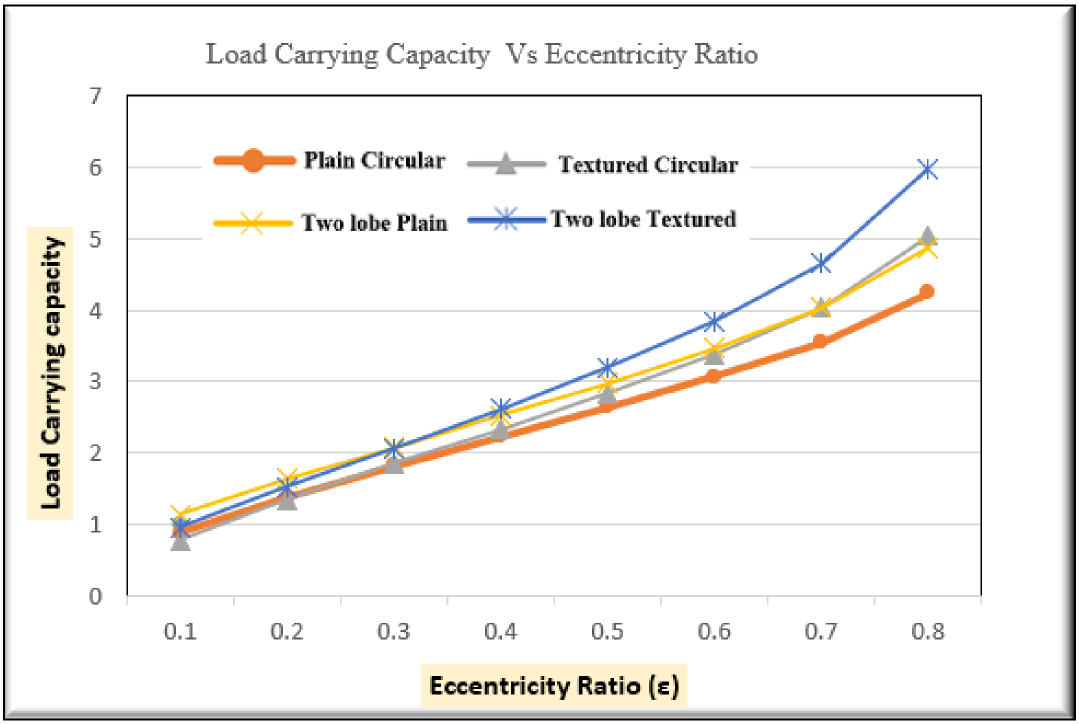

Figure 4: Variation of load carrying capacity ($\bar{F}_0$) versus eccentricity ratio (ε).

3.2 Maximum fluid–film pressure ($\bar{P}_{max}$).

Figure 5. shows the variation of non-dimensional value of maximum fluid–film pressure ($\bar{P}_{max}$) of plain/textured circular and two lobe journal bearing against eccentricity ratio (ε). The value of maximum fluid-film pressure increases with the increment in the values of eccentricity ratio (ε) for both plain and textured journal bearings. There is a change in the thickness of fluid-film due to the presence of textures on the bearing surface, which increases the hydrodynamic lift.

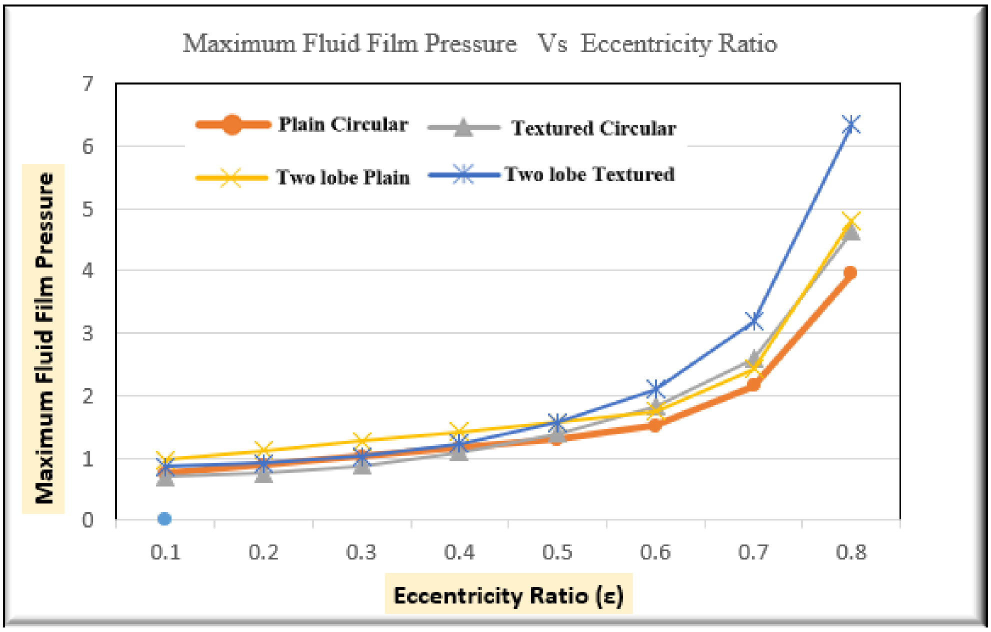

Figure 5: Variation of maximum fluid-film pressure ($\bar{P}_{max}$) versus eccentricity ratio (ε)

3.3 Lubricant flow rate ($\bar{Q}$).

Figure 6 : shows the variation of non-dimensional value of lubricant flow rate ($\bar{Q}$) of plain/textured journal bearings versus eccentricity ratio (ε). For the chosen value of eccentricity ratio (ε) 0.3, the non-dimensional value of lubricant flow rate ($\bar{Q}$) less than plain journal bearing.

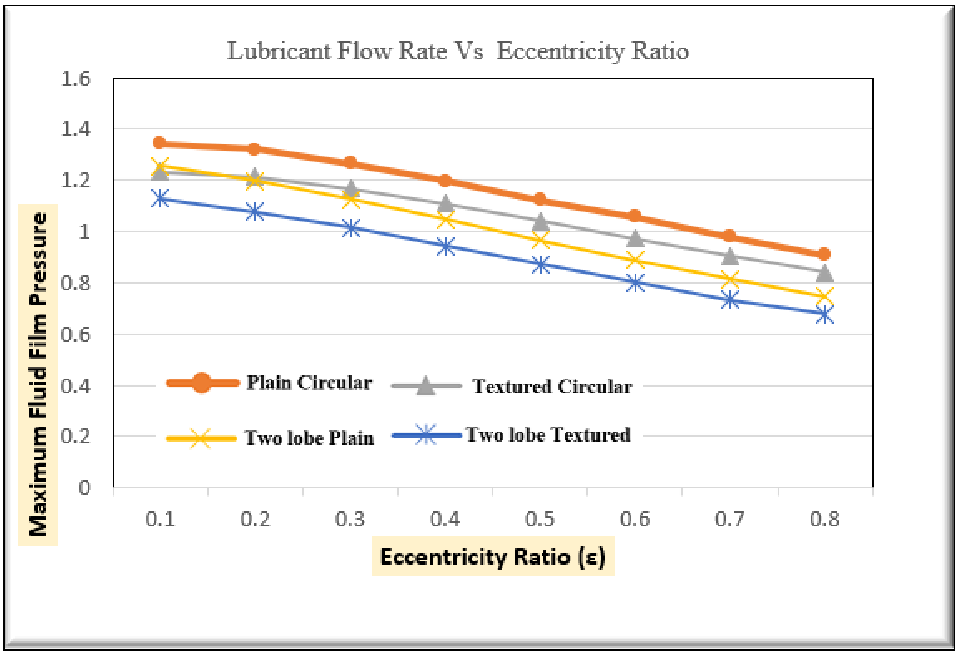

Figure 6: Variation of lubricant flow rate ($\bar{Q}$) versus Eccentricity ratio (ε).

3.4 Coefficient of fluid–film friction ($\bar{f}$).

The variation in the non-dimensional value of coefficient of fluid–film friction ($\bar{f}$) versus eccentricity ratio (ε) of plain/ textured journal bearings is shown in figure 7. It is observed that the coefficient of fluid-film friction of textured journal bearing is less than plain journal bearing. It is because of the reason that the surface textures store extra lubricant and serves as a reservoir during starved conditions and hence reduce the fluid-film friction.

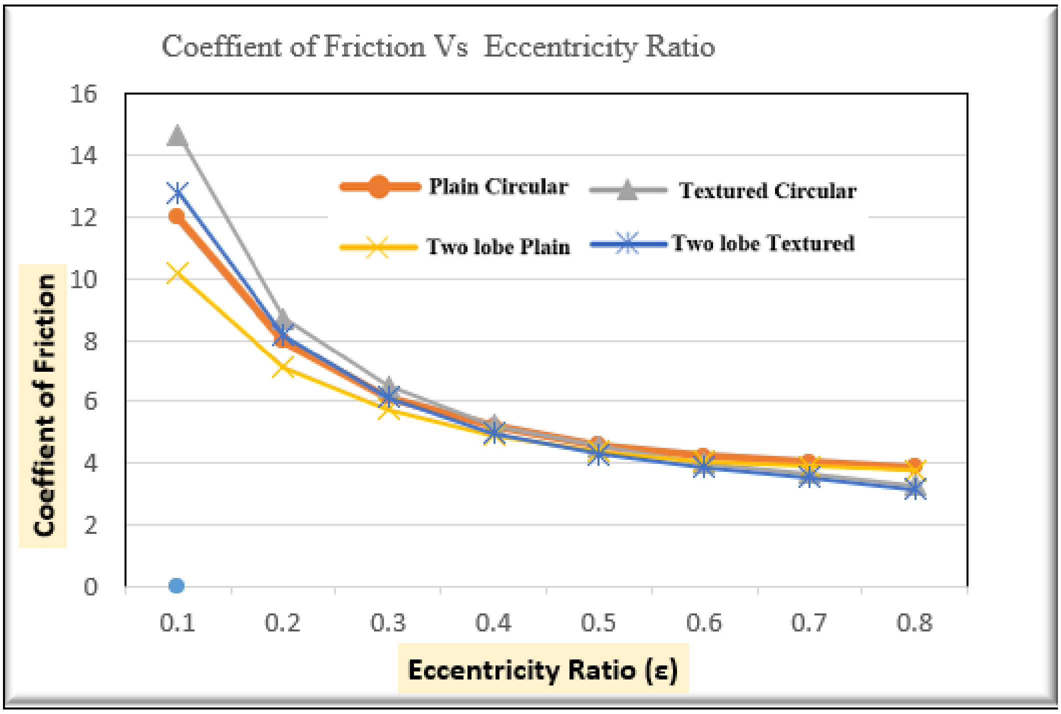

Figure 7: Variation of coefficient of fluid-film friction ($\bar{f}$) versus Eccentricity ratio (ε)

3.5 Fluid film Stiffness coefficient ($\bar{S}_{11}, \bar{S}_{22}$).

The fluid–film stiffness and damping coefficients are very important bearing characteristics parameters for the design of dynamically loaded journal bearing. figure 8 and figure 9 show the variation of non-dimensional values of direct fluid film stiffness coefficients ($\bar{S}_{11}, \bar{S}_{22}$) against the eccentricity ratio for a plain/textured journal bearing configurations. The textured journal bearing shows slight improvement in the non-dimensional value of direct fluid–film stiffness coefficient ($\bar{S}_{11}$) in horizontal direction and significant improvement in the non-dimensional value of fluid–film stiffness coefficient ($\bar{S}_{22}$) in vertical direction than plain journal bearing at relatively low value of eccentricity ratio

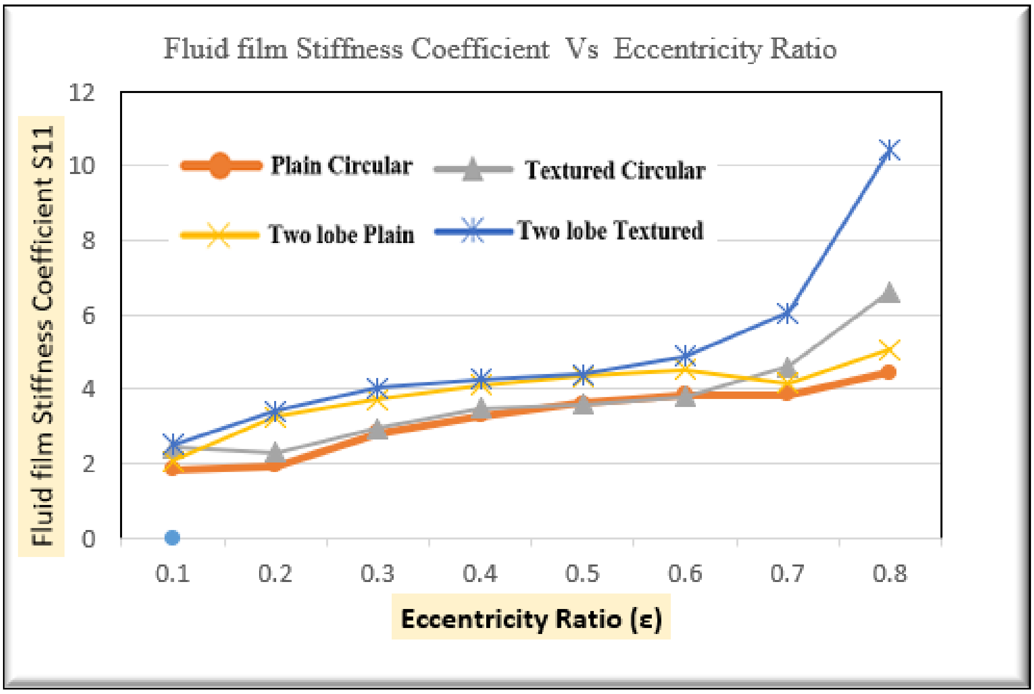

Figure 8: Variation of fluid-film stiffness coefficient fluid-film friction ($\bar{S}_{11}$) versus Eccentricity ratio (ε).

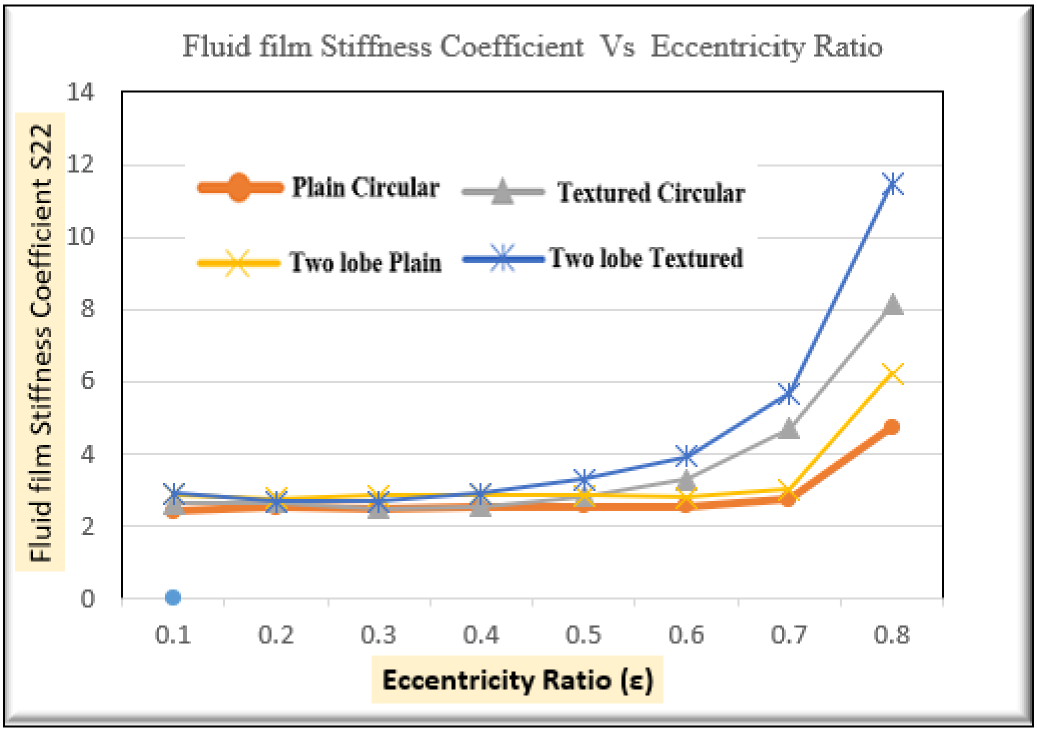

Figure 9: Variation of fluid-film stiffness coefficient fluid-film friction ($\bar{S}_{22}$) versus Eccentricity ratio (ε).

3.6 Fluid film damping coefficient ($\overline{C}_{11}, \overline{C}_{22}$).

The variation in the non-dimensional values of direct fluid–film damping coefficients ($\overline{C}_{11}, \overline{C}_{22}$) in horizontal and vertical directions of plain/textured journal bearings with the eccentricity ratio has been depicted in figure 10 and figure 11, respectively. The non-dimensional value of direct fluid–film damping coefficient ($\overline{C}_{11}, \overline{C}_{22}$) in vertical and horizontal direction increases with eccentricity ratio.

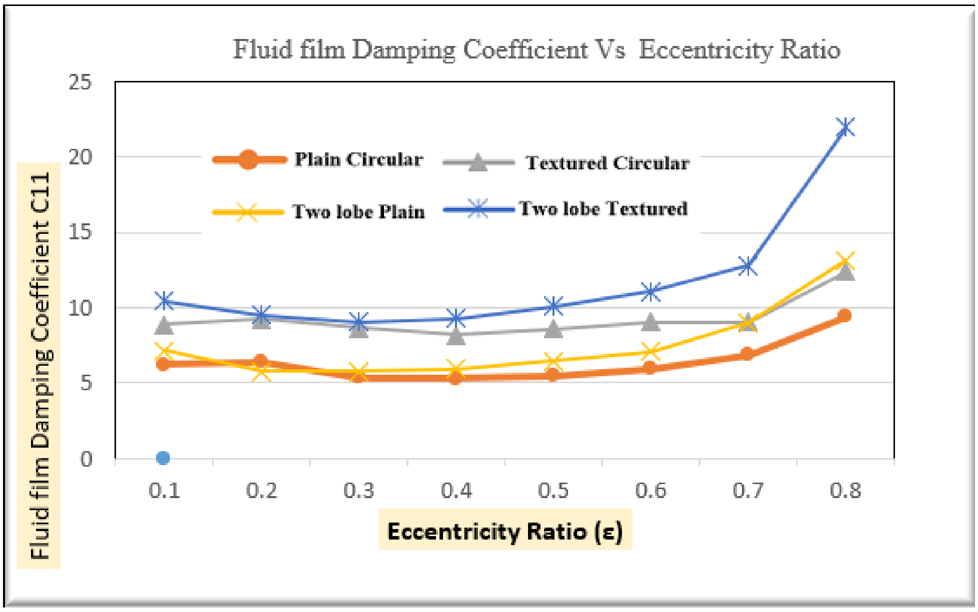

Figure 10: Variation of fluid-film damping coefficient fluid-film friction ($\overline{C}_{11}$) versus Eccentricity ratio (ε).

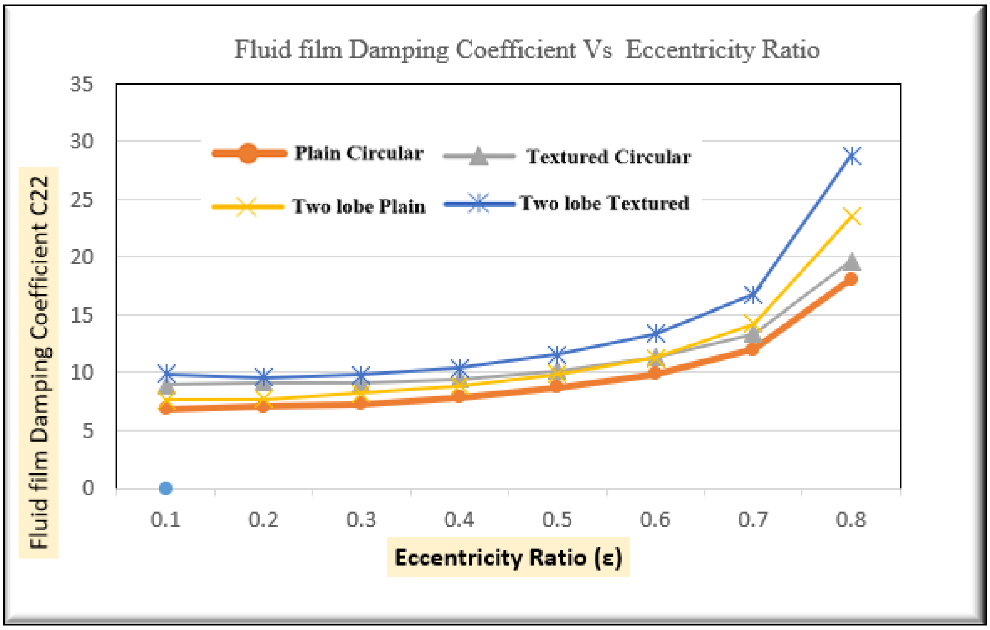

Figure11: Variation of fluid-film damping coefficient fluid-film friction ($\overline{C}_{22}$) versus Eccentricity ratio (ε)

4. CONCLUSIONS

The major conclusions on static and dynamic performance characteristics of textured two lobe journal bearing are as follows:

(1) The load carrying capacity ($\bar{F}_0$) of textured journal bearings is greater than plain journal circular and plain two lobe bearing because of the change in fluid-film thickness of lubricant due to the presence of textures on the bearing surface, which in turn increases the hydrodynamic lift.

(2) The presence of textures on the bearing surface reduces the value of coefficient of fluid film friction of journal bearing for both circular and two lobe configuration.

(3) Significant improvements in the dynamic characteristics of hydrodynamic journal bearings can be obtained by providing a texture on the bearing surface.

ACKNOWLEDGEMENTS

The authors would like to thank the anonymous reviewers and the editor for their very helpful suggestions to improve the manuscript.

DECLARATION OF INTEREST STATEMENT

The author(s) declared no potential conflicts of interest with respect to the research, authorship, and/or publication of this article.

REFERENCES

[1] Tala-Ighil N, Fillon M, Maspeyrot P, et al. “Effects of surface texture on journal-bearing characteristics under steady-state operating conditions”, Proc IMechE, Part J: J Engineering Tribology, 221, 2007, pp.623-633.

[2] Tala-Ighil N, Fillon M and Ma0speyrot P. “Effect of textured area on the performance of hydrodynamic journal bearing” Tribol Int, (44), 2011, pp.211-219.

[3] Daniel Gropper n, Ling Wang, Terry J. Harvey, “Hydrodynamic lubrication of textured surfaces: A review of modeling techniques and key findings”, Tribology Int., (94), 2016, pp. 509-529.

[4] Niranjan Singh and RK Awasthi, “Influence of dimple location and depth on the performance characteristics of the hydrodynamic journal bearing system”, Proc IMechE Part J: J Engineering Tribology, 2020, pp. 1-14

[5] Nacer Tala-Ighil, Michel Fillon, “A numerical investigation of both thermal and texturing surface effects on the journal bearings static characteristics”, Tribology International, 2015, pp.1-48.

[6] Tayal, S. P., Sinhasan, R. and Singh, D. V “Analysis of hydrodynamic journal bearings having non-Newtonian lubricants”,Tribology Inter,1982, pp. 17-21.

[7] L. Roy and S. K. Laha, “Steady state and dynamic characteristics of axial grooved journal bearings,” Tribol. Int., vol. 42(5), 2009, pp. 754-761.

[8] H. Adatepe, A. Bykloglu, and H. Sofuoglu, “An investigation of tribological behaviors of dynamically loaded non-grooved and micro-grooved journal bearings,” Tribol. Int., vol. 58, 2013, pp. 12–19.

[9] A. B. Shinde and P. M. Pawar, “Effect of partial grooving on the performance of hydrodynamic journal bearing,” Ind. Lubr. Tribol., Vol. 69(4), 2017, pp. 574-584.

[10] Raimondi, J. Boyd, "A solution for the finite journal bearing and its application to analysis and design," Part-I, II, III, Trans. ASLE, Vol.-I,II,III,1956,1957, pp. 159-174, 175-193, 194-203.

[11] J. Bouyer and M. Fillon, "Experimental measurement of the friction torque on hydrodynamic plain journal bearings during start-up," Tribology Int., Vol.44, 2011, pp. 772-781.

[12] Baril D. O., Quinzani L. M. Vignolo G. Gustavo., "Approximate analytical solution to Reynolds equation for finite length journal bearings," Tribology International Vol 44, 2011, pp. 1089-1099.

[13] Jin Chen and Sinan H. Hussain Xiaoping Pang, "Numeric And Experimental Study Of Generalized Geometrical Design of a Hydrodynamic Journal Bearing Based on the General Film Thickness Equation," Journal of Mechanical Science and Technology 26 (10), 2012,pp. 3149-3158.

[14] F. T. Barwell, “Hydrodynamic lubrication and its implication for journal bearing design”, A.S.N.E. Journal, 1959, pp. 505 -510.

[15] P.C. Warner, “Static and dynamic properties of partial journal bearings”, Trans. ASME, J. Basic Eng., 1963, pp. 247-255

[16] S. M. Metwalli, G. S. A. Shawki, M.O. A. Mokhtar, M.A.A. Seif, “Multiple design objectives in hydrodynamic journal bearing optimization”, Vol.106, 1984,pp. 54-60.

[17] G. Capone, V. Aogstino and D. Guide , “A finite length plain journal baring theory”, Trans. ASLE, Vol.116,1994, pp.648-653.

[18] H. Hirani, T V V L N. Rao, K. Athre, S. Biswas, “Rapid performance evaluation of journal bearings”, Trib. Inter., Vol.30 (11), 1997, pp. 825-834.

[19] H. Hashimoto and K. Matsumoto, “Improvement of Operating Characteristics of High-Speed Hydrodynamic Journal Bearings by Optimum Design Part - I”, Jour. of Trib., Vol. 123, 2001, pp. 305-312.

[20] C. B. Khatri and S. C. Sharma, Behaviour of two-lobe hole-entry hybrid journal bearing system under the combined influence of textured surface and micropolar lubricant, Ind. Lubr. Tribol., vol. 69, no. 6, Nov. 2017,pp. 844–862.

[21] X.-L. Wang and K.-Q. Zhu, Numerical analysis of journal bearings lubricated with micropolar fluids including thermal and cavitating effects, Tribol. Int., vol. 39, no. 3, Mar. 2006,pp. 227–237.

[22] R W Jakeman, "A numerical analysis method based on flow continuity for hydrodynamic journal bearings," Tribology Inter. Vol 17, 1984,pp. 325-333,

[23] Blancob C J C, Macedoc E N, Maneschya C E A, Quaresmac J N N Santosa E N, "Integral transform solutions for the analysis of hydrodynamic lubrication of journal bearings," Tribology Inter. Vol 52, pp. 161-169, 2012.

[24] Chasalevris A Sfyrisa D, "An exact analytical solution of the Reynolds equation for the finite journal bearing lubrication," Tribology Inter. Vol 55, pp. 46-58, 2012.

[25] Chasalevris A Sfyrisa D, "Evaluation of the finite journal bearing characteristics, using the exact analytical solution of the Reynolds equation," Tribology Inter. Vol. 57, pp. 216-234, 2013.

[26] Tayalt, S.P., Sinhasant, R. and Singht, D.V.,“Analysis of Hydrodynamic Journal Bearings having Non-Newtonian Lubricants (Prandtl Model) by A Finite Element Method”,Journal of Mechanical Engineering Science,IMechE, Vol.23(2), 1981, pp. 63-68.

[27] Rajalingham, C., Prabhu, B. S. and Rao, B. V. A. “The Steady State Performance of a Hydrodynamic”, Wear, vol. 55, 1979, pp. 107–120.

[28] H. Christensen and Tonder, K. “The Hydrodyamic Lubrication of Rough Journal Bearings”, Journal of Lubrication Technology, Transactions of the ASME,1973,pp.166-172

[29] S. T. N. Swamy, et.al. “Calculated Load Capacity of Non-Newtonian Lubricants in Finite Width Journal Bearings”, Wear,31, 1975, pp. 277-285.

[30] A. Harnoy, "Bearing design for machinery", Dekker Mechanical Engineering, 2002.

[31] G. Stachowiak and A.W. Batchelor, “Engineering tribology”, Elsevier ,2006

[32] M. M. Khonsari and E. R. Booser, "Applied tribology bearing design and lubrication", John Wiley & Sons Ltd., 2008

[33] W. B. Rowe, “Hydrostatic, Aerostatic, and Hybrid Bearing Design” Elsevier Publication, 2012.

[34] B. Bhushan, “Introduction to tribology”, A John Wiley & Sons Ltd.,2013

[35] M. K. Ghosh, B. C. Majumdar and M. Sarangi, “Fundamentals of Fluid Film Lubrication” McGraw-Hill, 2014.

[36] H. Hirani, “Fundamentals of engineering tribology with applications”, Cambridge university press, 2016.

[37] Amit Chauhan, “Non- circular Journal Bearing” Springer Briefs in Materials, Springer Briefs, 2016.

[38] Yukio Hori, “Hydrodynamic Lubrication” springer-verlag, 2006.

NOMENCLATURE

a_b	bearing land width (mm)
c	radial clearance (mm)
C_{ij}	damping coefficients (i, j = x, z OR 1, 2) (N-s-mm^2)
D	journal diameter (mm)
e	journal eccentricity (mm)
E	modulus of elasticity (MPa)
F	fluid film reaction
F_x, F_z	X and Z components of fluid film reactions $\partial h / \partial t \neq 0$ (N)
F_0	fluid film reaction $\partial h / \partial t = 0$ (N)
g	gravitational acceleration (m-s^2)
h	local fluid-film thickness (mm)
h_r	reference fluid film thickness (mm)
h_p	dimple depth (mm)
$h_{\min}$	minimum fluid film thickness (mm)
L	bearing length (mm)
p	pressure (MPa)
p_s	supply pressure (MPa)
p_c	pressure at holes (MPa)

Q	bearing volume flow rate (mm^2 -s^{-1})
R_j	radius of journal, mm
R_b	radius of bearing (mm)
r_p	base radius of dimple (mm)
S_{ij}	stiffness coefficients (i, j = x, z OR 1, 2), N-s-mm^2
t	time (s)
W_0	external load (N)
x_l, z_l	local Cartesian coordinates of dimple
X, Y, Z	Cartesian coordinates
$X_{J,} Z_{J,}$	journal center coordinates (mm)
M_c	critical mass of journal (kg)
M_J	journal mass (kg)
ω_J	journal rotational speed (rad/s)
ω_{th}	threshold speed (rad/s)

Non-dimensional parameters

$\bar{a}_b$	$\frac{a_b}{L}$, land width ratio
$\bar{C}_{ij}$	$C_{ij}\left(c^3 / \mu R_J^4\right)$
$(\bar{F}, \bar{F}_0)$	$(F, \bar{F}_0) / p_s R_J^2$
$\bar{h}$	$(h)/c$
$\bar{h}_p$	$(h_p)/c$
$\bar{M}_J, \bar{M}_c$	$\left(M_c, M_J\right)\left(\frac{c^2 p_s}{\mu R_J^2 \omega_J}\right)$
$\bar{p}, \bar{p}_c, \bar{p}_{\max}$	$\left(p, p_c, p_{\max}\right) / p_s$
$\bar{Q}$	$Q(\mu / c^3 p_s)$
$\bar{r}_p$	r_p / c
$\bar{S}_{ij}$	$S_{ij}\left(c / p_s R_J^2\right)$
$\bar{W}_0$	$W_0 / p_s R_J^2$
$\left(\bar{X}_J, \bar{Z}_J\right)$	$\left(X_J, Z_J\right)/c$
α, β	$(X, Y)/R_J$ circumferential and axial coordinates
$\bar{\dot{\gamma}}$	$\dot{\gamma}\left(\mu_r R_J / c p_s\right)$
δ	c_1 / c_2, offset factor
$\bar{\delta}$	dimensionless dimple radius
ε	e/c, eccentricity ratio
$\bar{\omega}_{th}$	ω_{th} / ω_I
$\bar{\tau}$	$\tau(R_J / c p_s)$
Ω	$\omega_J(\mu R_J^2 / c^2 p_s)$, speed parameter

Matrices and vectors

$\left[\overline{F}\right]$	= Fluidity matrix;
$[N]$	= Shape function matrix;
$\{\overline{p}\}$	= Nodal pressure vector;
$\{\overline{Q}\}$	= Nodal flow vector
$\{\overline{R}_x, \overline{R}_z\}$	= Nodal RHS vectors due to journal center velocity; and
$\{\overline{R}_H\}$	Colum vector due to hydrodynamic terms.

Subscripts and superscripts

$\bar{}$	= Non-dimensional parameters;
b	= Bearing;
J	= Journal;
r	= Reference value;
x, y, z	= Components in X,Y and Z directions; and
	= First derivative w.r.t. time.

Citation: Kushare Dnyaneshwar V and Soni Sandeep. (2025). Performance Analysis of Surface Textured Hydrodynamic Journal Bearing under Influence of Non-Newtonian Lubricant. International Journal of Mechanical Engineering and Technology (IJMET), 16(3), 67-87.

Abstract Link: https://iaeme.com/Home/article_id/IJMET_16_03_004

Article Link:
https://iaeme.com/MasterAdmin/Journal_uploads/IJMET/VOLUME_16_ISSUE_3/IJMET_16_03_004.pdf

✉ **editor@iaeme.com**